Contents lists available at GrowingScience

International Journal of Industrial Engineering Computations

homepage: www.GrowingScience.com/ijiec

Green pickup and delivery problem with private drivers for crowd-shipping distribution considering traffic congestion

Xue Wu[a], Dawei Hu[a*] and Tianyang Gao[a]

[a]*School of Transportation Engineering, Chang'an University, Xi'an 710064, China*

C H R O N I C L E

Article history:
Received March 15 2024
Received in Revised Format September 16 2024
Accepted October 18 2024
Available online October 18 2024

Keywords:
Crowd-shipping
PM and NOx emissions
Green pickup and delivery problem
Congestion
Improved adaptive large neighborhood search

A B S T R A C T

Crowd-shipping, employing private drivers to partially replace company-owned trucks in distribution, has emerged as a prominent trend for its cost-effectiveness and sustainability. While crowd-shipping is known as a distribution pattern that combines economic efficiency and environmental benefits, however, the frequent occurrence of traffic congestion has made this pattern less effective than it should be. In this research, the problem of vehicle routing optimization under traffic congestion is investigated from the perspective of simultaneously reducing environmental pollution and costs. Considering private drivers picking up and delivering parcels on the way, this study incorporates the objective of minimizing transport as well as particulate matter (PM) and nitrogen oxides (NOx) emission costs into route optimization for crowd-shipping and proposes a Green Pickup and Delivery Problem with Private Drivers (GPDP-PD). To be more realistic, vehicle speeds depend on the level of traffic congestion, reflecting the time-dependent nature of the proposed model. An improved adaptive large neighborhood search (ALNS) algorithm is developed, and computational experiments are conducted to demonstrate the efficiency of the improved ALNS. Case studies show that there is uncertainty about the environmental benefits of crowd-shipping under traffic congestion. Our proposed model is capable of efficiently allocating private drivers and optimizing vehicle routes according to road conditions, thus identifying the crowd-shipping operational scheme with the lowest cost and emissions. Moreover, a time limit of 0.7-0.8 h and the low cost of private drivers can achieve environmental and economic benefits simultaneously. It provides useful insights into the sustainability of logistics and distribution.

1. Introduction

Given the exploding demand for parcel distribution and the challenges associated with environmentally friendly freight mobility in urban areas (Ghaderi et al., 2022; Punel & Stathopoulos, 2017; Rafael et al., 2023), a growing number of solutions have emerged. One type of solution widely adopted by Amazon, Walmart, and JD.com is crowd-shipping, i.e., getting ordinary people (private drivers), who have an original travelling schedule, to take a detour to pick up and deliver parcels for a small amount of compensation (Dahle et al., 2019; Peng et al., 2024). Traditional distribution generally only uses company-owned trucks to serve customers, causing significant on-road NO_x and PM emissions (Meyer et al., 2019). Crowd-shipping, which utilizes private drivers already on the road to partially replace heavy trucks for customer service, is a promising way to reduce total freight costs and emissions simultaneously (Bortolini et al., 2022; Le et al., 2019). To leverage the benefits of crowd-shipping, our study focuses on achieving the cost-saving objective of environment-friendly routing and assessing the environmental impact of crowd-shipping by monetizing emissions such as PM and NO_x. Non-exhaust PM emissions are mainly affected by vehicle miles travelled (VMT). NO_x and exhaust PM emissions are influenced by fuel consumption. In

* Corresponding author
E-mail dwhu@chd.edu.cn (D. Hu)
ISSN 1923-2934 (Online) - ISSN 1923-2926 (Print)
2025 Growing Science Ltd.
doi: 10.5267/j.ijiec.2024.10.006

fact, both fuel consumption and vehicle miles travelled are influenced by varying speeds. Hence, to approximate a realistic emission pattern, the congestion index and triangular distribution are applied to simulate the speed variation due to changes in traffic conditions.

The contributions to the literature of our research can be summarized as follows. Prior research has concentrated on the economic effects of crowd-shipping (Dahle et al., 2019; Le et al., 2019; Peng et al., 2024). We consider the environmental effects of PM and NO_x in crowd-shipping and measure such an impact by monetizing different pollutants. Moreover, vehicle speed has a great impact on emissions generated during crowd-shipping operations, but it tends to vary with traffic conditions. Therefore, our study incorporates real-time vehicle speed variations into crowd-shipping to accurately measure the emissions generated during the distribution. Specifically, the green pickup and delivery problem with private drivers (GPDP-PD) is developed that incorporates both PM and NO_x emissions into the route optimization while accounting for the impact of a heterogeneous fleet with non-constant speeds on the emissions to closely simulate real-world conditions. Besides, an improved adaptive large neighborhood search (ALNS) is proposed to solve the GPDP-PD. In addition, a case study provides some insights into operating a crowd-shipping service.

2. Literature review

Our proposed GPDP-PD is an extension of classical pickup and delivery problems, aiming to optimize the distribution cost while taking into account other factors including PM and NO_x emissions, private drivers, and varying speed. The relevant research is discussed as follows.

2.1 Pickup and delivery problem with private drivers

Since Archetti et al. (2016) first proposed a crowd-shipping system involving private drivers and company-owned trucks, it has been considered to be one of the important topics for future research in areas associated with distribution and e-commerce (Boysen et al., 2022; Le et al., 2019). In Archetti et al. (2016), the vehicle routing problem with occasional drivers (VRPOD) was developed. The objective of the problem was to optimize routes at low cost for occasional drivers (private drivers) and company-owned trucks. Each private vehicle was allowed to serve a specific customer within a limited time. To ensure all orders can be covered, using only private drivers might not be sufficient. Therefore, trucks were also licensed to serve customers as supplementary to private driver delivery. Based on Archetti et al. (2016), Dahle et al. (2019) extended VRPOD to the pickup and delivery problem with time windows and occasional drivers (PDPTW-OD), demonstrating the cost-saving potential of crowd-shipping in a pickup and delivery scenario. Tao et al. (2023) proposed a multi-depot pickup and delivery vehicle routing problem with dynamic private drivers, where all drivers start at the depot. The numerical experiments show that the level of customer service can be greatly enhanced by the involvement of private drivers in distribution. Moreover, numerous models with the objective of minimizing economic costs have been motivated by considering factors that have a great impact on crowd-shipping route selection including time window, transshipment, and stochastic delivery locations (Archetti et al., 2021; Macrina et al., 2020; Su et al., 2023). However, these studies have predominantly focused on the economic benefits of crowd-shipping, while largely overlooking its environmental impact.

2.2 Green vehicle routing problem

With the widespread interest in sustainable development, the vehicle routing problem (VRP) has been extended to the green vehicle routing problem (GVRP), with the objective of considering environmental impacts. One of the earliest studies is Kara et al. (2007). The authors incorporated fuel consumption objectives into the VRP and found that a variety of factors including vehicle load, vehicle weight, and time spent, etc., can affect the energy consumption for travelling over a given distance. Bektas & Laporte (2011) extended the VRP to the pollution-routing problem by considering fuel, travel distance, greenhouse gas emissions, and other costs in the objective. Cirovic et al. (2014) proposed the GVRP of light delivery trucks in urban areas, concentrating on reducing toxic exhaust emissions including SO_2, NO_x, CO, $PM_{2.5}$, etc. Lou et al. (2024) developed the vehicle routing model with the objective of minimizing CO_2 emissions and proposed a hybrid genetic algorithm to solve the model.

In our study, we focus only on the impact of crowd-shipping on NO_x and PM reduction, as they are emissions from the transport sector that are projected to increase and have a direct impact on health in the coming years (Michiels et al., 2012). The first step in integrating emissions into the objective function of GVRP is to quantify exhaust PM emissions and NO_x, which are primarily from fuel combustion. Barth et al. (2005) developed the comprehensive modal emissions model (CMEM) which covers all important factors of vehicle fuel consumption. Many researchers have used CMEM to estimate emissions from distribution and to model GVRP mathematically. Niu et al. (2018) integrated CMEM into a mixed open GVRP to assess the emissions. The results showed that the CMEM model effectively calculates the emissions generated during vehicle travelling. Wu & Dong (2023) investigated the eco-routing problem considering deterioration and fuel consumption calculated by the CMEM during the transport of perishables, but the vehicle speed was set as a constant. Except for NO_x and exhaust PM emissions, Rexeis and Hausberger (2009) indicated that non-exhaust emissions contribute to 90% of PM emissions from transportation. To accurately measure PM from the transport sector, different pollution measurement models were developed to test the non-exhaust emissions emitted by different vehicle types (Grigoratos et al., 2023; Liu et al., 2021; Timmers et al.,

2016). Although PM emissions from non-exhaust sources account for a significant proportion of PM emissions, there is no literature that takes this into account in GVRPs for route optimization.

2.3 *Speed varying*

Generally, the vehicle speed does not remain constant due to the uncertainty of road conditions. To approximate the speed variations of a vehicle in reality, the entire planning time period is split into several short time segments, and the vehicle speed within each time segment is regarded as constant (Ichoua et al., 2003). Many studies have been conducted on this basis. Yao et al. (2019) employed road traffic state indexes to describe the real-time variation of traffic congestion and investigated the influence of such variations on vehicle routing optimization. Poonthalir & Nadarajan (2018) described varying speeds using a triangular distribution. Then, the authors studied GVRP in a congested environment and the results showed that a reasonable routing plan with the objective of minimizing fuel consumption can be achieved when the varying speed was taken into account. Chen et al. (2021) used the traffic congestion index to depict the level of congestion and developed a time-dependent GVRP from a low-carbon economy perspective. However, it is unfortunate that the traffic congestion index only takes into account the variation of vehicle speeds under congested conditions, whereas, in reality, vehicle speeds are not constant even under unimpeded traffic conditions. Luo et al. (2024) studied a GVRP with the goal of minimizing carbon emissions considering time-varying traffic congestion and developed a branch-price-and-cut (BPC) algorithm to solve the model.

From the literature review, few of the previous research discussed crowd-shipping routing optimization considering real-world speed variations and emissions except for Hla et al. (2019). Different from most of the previous research on VRPOD, Hla et al. (2019) incorporated an energy consumption model into the crowd-shipping route optimization. However, they simplified the energy consumption to a linear function related only to distance. Poonthalir & Nadarajan (2018) integrated variable speed into the classical VRP problem by using a triangular distribution to simulate varying speeds during traffic congestion. Compared to Hla et al. (2019), the setting that varying speeds have different effects on fuel consumption is more realistic in Poonthalir & Nadarajan (2018). However, Poonthalir & Nadarajan (2018) only addressed the homogeneous vehicle delivery problem and the fuel consumption model did not take into account many practical factors such as vehicle type, vehicle weight, etc. Moreover, private drivers were not involved in deliveries, hence the time constraint and drivers' original journeys were also ignored. To fill these gaps, our study considers the time-dependent nature of vehicle speeds in different traffic conditions and integrates an energy consumption model that takes varying speeds into account in GPDP-PD. In addition, the heterogeneous fleet, original journeys by private drivers, and simultaneous pickup and delivery are also involved in our proposed model simultaneously. Then for the solution method, we develop an improved Adaptive Large Neighborhood Search (ALNS) algorithm to solve GPDP-PD efficiently and obtain managerial insights through a case study on several key factors to offer some useful insights for related logistics enterprises.

3. Problem description

The GPDP-PD can be defined on a complete graph $G = (N, A)$, where $N = P \cup D \cup O \cup S \cup \{0\}$ denotes the set of all points and A denotes the set of arcs. $\{0\}$ denotes the depot. $C = P \cup D$ includes the set of pickup points $P = \{1, 2, ..., n\}$ and the set of delivery points $D = \{n+1, n+2, ..., 2n\}$. l_i represents the service demand at point i. Service request for customer i consists of serving a quantity from pickup point i to delivery point $n+i$, where $l_{n+i} = -l_i$. Let the set of vehicles $K = T \cup R$. A fleet of company-owned trucks T and a fleet private drivers R are available to serve customers. $N_v = O \cup S$ represents the set of origins $O = \{1, 2, ..., m\}$ and the set of destinations $S = \{m+1, m+2, ..., 2m\}$ of the private drivers. $O(r)$ and $S(r)$ denote origin and destination of private driver r, respectively. The set of pollutant types emitted by vehicles is Z, $Z = \{1, 2, ..., z\}$.

Fig. 1 illustrates an example of crowd-shipping containing one depot, four private drivers, two trucks, and six customers. Customer requests can only be picked up before delivered. The private drivers selected by the crowd-shipping company start at their origins, serve specified customers, and then return to the corresponding destinations, otherwise, they travel directly from their origins to the destinations. Trucks are used as a supplement to private driver distribution, all departing from and ending at the depot. The relevant symbols defined in this paper are shown in Table 1.

Table 1
Parameters and variables of the GPDP-PD.

Parameters and intermediate variables	
d_{ij}	Distance between point i and point j
t_{ik}^{A}	Time for vehicle k to arrive at point i

t_{ik}^{L}	Time for vehicle k to departure of point i
c_t	Transport cost per unit of time for company-owned truck t
c_r	Transport cost per unit of time for private driver r
p_z	Emission cost per unit of pollutant z emitted
E_{ijk}^{z}	Exhaust emissions of pollutant z from point i to point j of vehicle k
NE_{ijk}^{z}	Non-exhaust emissions of pollutant z from point i to point j of vehicle k
T_0	Departure time of company-owned trucks from depot 0
T_r	Departure time of private driver r from its origin
TL_r	Time limit for vehicle r to reach its destination
st_i	Service duration at point i
f_{ij}	Vehicle load from point i to point j
Q_k	Capacity of vehicle k
ε_r	The quality of goods that private driver r would have been required to carry from its origin to its destination
l_i	Demand of point i
m	A large positive integer
Decision variables	
x_{ijt}	Binary variable indicating whether arc (i, j) is travelled by company-owned truck t
y_{ijr}	Binary variable indicating whether arc (i, j) is travelled by private driver r

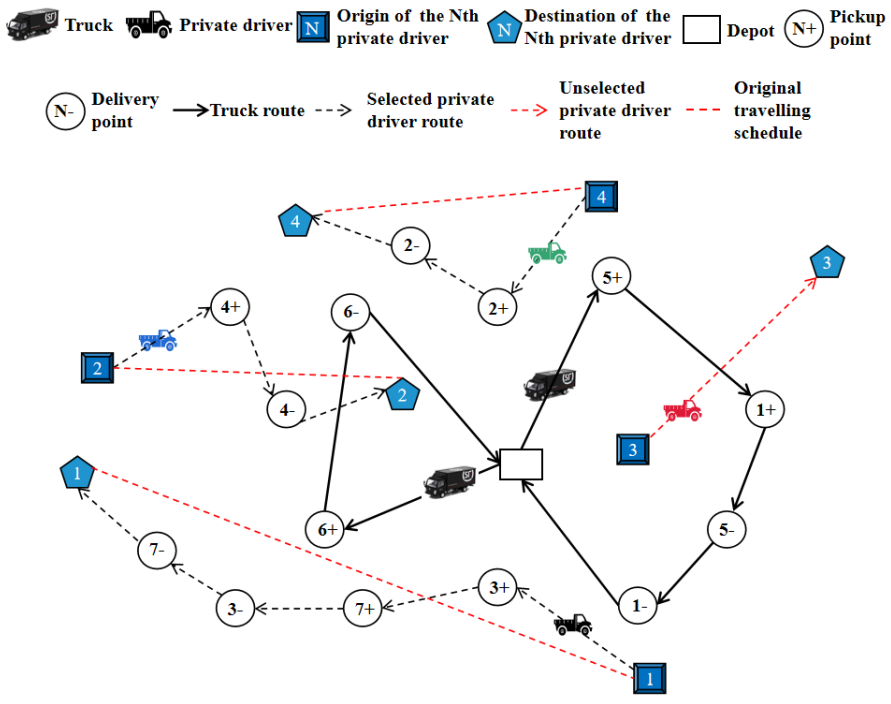

Fig. 1. Routes illustration of the GPDP-PD.

4. Model development

4.1 Travel time analysis

4.1.1. Speed under congested and unimpeded traffic conditions

Based on massive vehicle trajectory and location data, China's real-time traffic detection application, Baidu Map, developed the congestion index to measure the degree of traffic congestion within the city. The congestion index is calculated as the ratio

of the actual travel time to the minimum unimpeded travel time. When the congestion index is less than 1.5, the road is unimpeded; otherwise, the larger the congestion index, the more severe the congestion. Vehicle speeds are consistent in congestion; however, this is not the case under unimpeded traffic. In terms of speeds when the congestion index is less than 1.5, vehicles are usually unlikely to be travelling at a maximum speed. The triangular distribution, a useful tool in subjectively estimating variables, is used to estimate vehicle speeds under unimpeded traffic conditions. A triangular distribution is a continuous probability distribution with the most likely value p, the minimum possible value m, and the maximum possible value n and where $m < n$ and $m \le p \le n$. The probability density function of the triangular distribution is shown in Eq. (1).

$$f(x)=\begin{cases} 0 & x<m \\ \dfrac{2(x-m)}{(n-m)(n-p)} & m\le x<p \\ \dfrac{2(n-x)}{(n-m)(n-p)} & p\le x<n \\ 0 & x\ge n \end{cases} \tag{1}$$

Vehicles generally travel at a speed between the minimum speed and the maximum speed. Adapted by Poonthalir and Nadarajan (2018), we assume that when traffic conditions change from congested to unimpeded conditions (or unimpeded to congested conditions), the vehicle speed undergoes a three-stage variation. Then, unimpeded speed can be assessed by averaging the expected speed value of these three-stage variations. For example, if a vehicle is travelling from congestion to an unimpeded period, the speed of a vehicle just entering a period of light congestion is θ_l and the maximum speed limit is θ_u. The speed interval is assumed to be $[\theta_l, \frac{\theta_u+2\theta_l}{3}, \frac{2\theta_u+\theta_l}{3}, \theta_u]$, where the expected speed in each interval requires to be calculated. Taking the first speed interval $[\theta_l, \frac{\theta_u+2\theta_l}{3}]$ as an example, let θ be the most likely speed, and θ for each vehicle can be taken at random between $[\theta_l, \frac{\theta_u+2\theta_l}{3}]$. Then, the expected speed $E(X)$ of the first speed interval $[\theta_l, \frac{\theta_u+2\theta_l}{3}]$ is calculated as Eq. (2).

$$E(X)=\int_{\theta_l}^{\frac{\theta_u+2\theta_l}{3}} xf(x)d(x)=\int_{\theta_l}^{\theta} x\frac{2(x-\theta_l)}{(\frac{\theta_u+2\theta_l}{3}-\theta_l)(\theta-\theta_l)}d(x)+\int_{\theta}^{\frac{\theta_u+2\theta_l}{3}} x\frac{2(\frac{\theta_u+2\theta_l}{3}-x)}{(\frac{\theta_u+2\theta_l}{3}-\theta_l)(\frac{\theta_u+2\theta_l}{3}-\theta)}d(x) \tag{2}$$

4.1.2. Travel time formulation

In case of a time-varying network, the travelling time of the vehicle from point i to point j can be divided into several time periods. D_h is the congestion index of a road from point i to point j at time period h, v_0 is the speed of a vehicle under the unimpeded condition, v_1 is the maximum speed limit, T_h is the end time of the period h. z_h is binary variable and equals to 1 when the road is unimpeded at time period h. Let $v'=v_0+(v_1D_h-v_0)z_h$, then the time of travelling from point i to point j from that road can be calculated using equations (3)-(5). If there are several links (roads) to reach point j from point i, we choose the one with the smallest value of t_{jk}^A.

(1) When vehicle k travels from point i to point j within a time period h, the travel time is formulated as follow:

$$t_{jk}^A-t_{ik}^L=\frac{d_{ij}}{v'}D_h \tag{3}$$

(2) When vehicle k travels from point i to point j across two time periods h and $h+1$, the travel time is formulated as follow:

$$t_{jk}^{A}-t_{ik}^{L}=T_h-t_{ik}^{L}+\frac{d_{ij}-\frac{v'(T_h-t_{ik}^{L})}{D_h}}{v'}D_{h+1} \tag{4}$$

(3) When vehicle k travels from point i to point j across more than two time periods and arrives at destination in the time period H, the travel time is formulated as follow:

$$t_{jk}^{A}-t_{ik}^{L}=T_h-t_{ik}^{L}+\sum_{r=1}^{H-1}(T_{h+r}-T_{h+r-1})+\frac{d_{ij}-\frac{v'(T_h-t_{ik}^{L})}{D_h}-\sum_{r=1}^{H-1}\frac{v'(T_{h+r}-T_{h+r-1})}{D_{h+r}}}{v'}D_{h+1} \tag{5}$$

4.1 NO_x and PM emission

NO_x and exhaust PM emissions are positively correlated with fuel consumption. Based on a fuel consumption model of Barth et al. (2005), if the effects of slope and acceleration are ignored, the fuel consumption F_{ijk} of vehicle k from point i to point j at a speed v can be calculated as:

$$F_{ijk}=\lambda\left(\frac{K_k N_k V_k d_{ij}}{v}+W_{ij}\gamma_k\alpha_k d_{ij}+\beta_k\gamma_k d_{ij}v^2\right) \tag{6}$$

where $\gamma_k=1/(1000n_{tfk}\eta)$, $\beta_k=0.5C_{dk}\rho A_k$, $\alpha_k=gC_{rk}$, $W_{ij}=M_k+f_{ij}$. The definitions and values of some of the parameters are shown in Table 2 (Cheng et al., 2017; Shi et al., 2020). The definitions and values of remaining parameters can be found in Cheng et al. (2017).

Table 2
Parameter definitions and values about fuel consumption.

Parameter	Description	Company-owned truck	Private driver 1	Private driver 2	Private driver 3
M_k	Curb weight (kg)	6328	6328	4672	1020
Q_k	Maximum payload (kg)	5080	5080	2585	555
K_k	Engine friction factor (kJ/rev/L)	0.20	0.20	0.25	0.20
N_k	Engine speed (rev/s)	33	33	39	47
V_k	Engine displacement (L)	5.00	5.00	2.77	2.89
C_{dk}	Coefficient of aerodynamics drag	0.60	0.60	0.60	0.60
C_{rk}	Coefficient of rolling resistance	0.01	0.01	0.01	0.01
A_k	Frontal surface area (m^2)	9.00	9.00	9.00	2.33
n_{tfk}	Vehicle drive train efficiency	0.45	0.45	0.40	0.34

Note: The number after "private driver" refers to different vehicle types

The NO_x and exhaust PM emissions from point i to point j of vehicle k can be computed using Eq. (7) based on the EMEP (2019).

$$E_{ijk}^{z}=\begin{cases}\alpha_{zk}F_{ijk} & if\ z \text{ is exhaust PM or } NO_x\\ 0 & if\ z \text{ is non-exhaust PM}\end{cases} \tag{7}$$

where z is the pollutant category, either NO_x, exhaust PM emissions or non-exhaust PM emissions and $z \in Z$. α_{zk} represents the emission factor of vehicle k for pollutant z, which can be found in Table 3. NO_x is only sourced from exhaust emissions, while PM is also present in non-exhaust emissions, which can be divided into brake wear, tyre wear, and road wear emissions. Based on the EMEP (2013), the non-exhaust emissions from point i to point j of vehicle k can be computed as follow:

$$NE_{ijk}^{z} = \begin{cases} \sum_{b \in B} \omega_{bk} d_{ij} & if\ z \text{ is non-exhaust PM} \\ 0 & if\ z \text{ is exhaust PM or } NO_x \end{cases} \tag{8}$$

where ω_{bk} denotes the non-exhaust emission factor of vehicle k for pollutant z from emission source b, which are listed in Table 3. $B = \{1, 2, ..., b\}$ is the non-exhaust emission source set including brake wear, tyre wear, and road wear emissions.

Table 3
The emission factor for NO_x, exhaust and non-exhaust PM emissions.

Category	Company-owned truck	Private driver 1	Private driver 2	Private driver 3
NO_x (g L^{-1})	24.14	24.14	14.91	8.73
Exhaust PM (g L^{-1})	0.030	0.030	0.025	0.020
Non-exhaust PM (Tyre wear and brake wear combined) (g km^{-1})	0.033	0.033	0.029	0.025
Non-exhaust PM (Road wear) (g km^{-1})	0.016	0.016	0.013	0.010

Note: Parameter values refer to EMEP (2013), EMEP (2019), and Liu et al. (2022); The number after "private driver" refers to different vehicle types

4.2 GPDP-PD model

The GPDP-PD is proposed as follow:

$$\begin{aligned} \min & \sum_{i \in C \cup 0} \sum_{j \in C \cup 0} \sum_{t \in T} c_t (t_{jt}^{A} - t_{it}^{L}) x_{ijt} + c_r [\sum_{i \in C \cup O} \sum_{j \in C \cup S} \sum_{r \in R} (t_{jr}^{A} - t_{ir}^{L}) y_{ijr} - \sum_{i \in O} \sum_{j \in S} \sum_{r \in R} (t_{jr}^{A} - t_{ir}^{L}) y_{ijr}] \\ & + \sum_{i \in C \cup 0} \sum_{j \in C \cup 0} \sum_{t \in T} \sum_{z \in Z} p_z (E_{ijt}^{z} + NE_{ijt}^{z}) x_{ijt} + \sum_{i \in C \cup O} \sum_{j \in C \cup S} \sum_{r \in R} \sum_{z \in Z} p_z (E_{ijr}^{z} + NE_{ijr}^{z}) y_{ijr} \\ & - \sum_{i \in O} \sum_{j \in S} \sum_{r \in R} \sum_{z \in Z} p_z (E_{ijr}^{z} + NE_{ijr}^{z}) y_{ijr} \end{aligned} \tag{9}$$

subject to

$$\sum_{\substack{i \in C \cup 0 \\ i \neq j}} \sum_{t \in T} x_{ijt} + \sum_{\substack{i \in C \cup O \\ i \neq j}} \sum_{r \in R} y_{ijr} = 1 \quad \forall j \in C \tag{10}$$

$$\sum_{i \in 0} \sum_{j \in C} x_{ijt} \leq 1 \quad \forall t \in T \tag{11}$$

$$\sum_{i \in 0 \cup C} \sum_{j \in C} x_{ijt} = \sum_{i \in 0 \cup C} \sum_{j \in C} x_{jit} \quad \forall t \in T \tag{12}$$

$$\sum_{i \in 0 \cup C} x_{ijt} = \sum_{i \in 0 \cup C} x_{jit} \quad \forall j \in C, t \in T \tag{13}$$

$$\sum_{j \in 0 \cup C} x_{ijt} - \sum_{j \in C} x_{j(i+n)t} = 0 \quad \forall i \in P, t \in T \tag{14}$$

$$y_{O(r)ir} = 1 \quad \forall i \in S(r) \cup C, r \in R \tag{15}$$

$$y_{iS(r)r} = 1 \quad \forall i \in O(r) \cup C, r \in R \tag{16}$$

$$\sum_{i \in C \cup O} y_{ijr} = \sum_{i \in C \cup S} y_{jir} \quad \forall j \in C, r \in R \tag{17}$$

$$\sum_{j \in D \cup C} y_{ijr} - \sum_{j \in C} y_{j(i+n)r} = 0 \quad \forall i \in P, r \in R \tag{18}$$

$$t_{0t}^{L} = T_0 \quad \forall t \in T \tag{19}$$

$$t_{ir}^{L} = T_r \quad \forall i \in O, r \in R \tag{20}$$

$$t_{ir}^{A} \le TL_r \quad \forall i \in S, r \in R \tag{21}$$

$$t_{it}^{L} \ge t_{it}^{A} + st_i - m(1 - x_{ijt}) \quad \forall i \in C \cup 0, j \in C \cup 0, t \in T \tag{22}$$

$$t_{ir}^{L} \ge t_{ir}^{A} + st_i - m(1 - y_{ijr}) \quad \forall i \in C \cup O, j \in C \cup S, r \in R \tag{23}$$

$$t_{ik}^{L} \le t_{(i+n)k}^{A} \quad \forall i \in P, k \in K \tag{24}$$

$$f_{ij} \le Q_t \sum_{t \in T} x_{ijt} \quad \forall i \in C, j \in C, t \in T \tag{25}$$

$$f_{ij} \le (Q_r - \varepsilon_r) \sum_{r \in R} y_{ijr} \quad \forall i \in C, j \in C, r \in R \tag{26}$$

$$f_{ij} = 0 \quad \forall i \in 0 \cup O, j \in C \tag{27}$$

$$\sum_{j \in C} f_{ji} - \sum_{j \in C} f_{ij} = l_i \quad \forall i \in C \tag{28}$$

$$x_{ijt}, y_{ijr} \in \{0,1\} \quad \forall i \in N, j \in N, t \in T, r \in R \tag{29}$$

The objective (9) minimizes the combination of company-owned truck transport costs, private driver transport costs, company-owned truck emission costs, and private driver emission costs. It is important to note that costs incurred by the unused private drivers need to be deducted from total costs. The monetary values of NO_x and PM emissions (i.e., p_z) can be found in Liu et al. (2022). Constraint (10) ensures that each point should be visited exactly once by a company-owned truck or private driver. Constraints (11)-(12) guarantee that each company-owned truck starts from the depot and returns to the same depot. Constraint (13) is the flow conservation constraint for company-owned trucks. Constraint (14) indicates that if a company-owned truck serves a pickup point, it has to serve the corresponding delivery point. Constraints (15)-(16) ensure that each private driver departs from its origin and returns to the corresponding destination. Constraint (17) is the flow conservation constraint for private drivers. Constraint (18) indicates that if a private driver serves a pickup point, it has to serve the corresponding delivery point. Constraints (19)-(23) track the change of time for each vehicle. Constraints (19) and (20) specify departure times for trucks and private drivers, respectively. Constraint (21) is a time limit for the private driver to reach the destinations. Constraint (22) traces the arrival time of the truck at point *j*, which is is simplified from $t_{jt}^{A} \ge t_{it}^{A} + st_i + t_{jt}^{A} - t_{it}^{L} - m(1 - x_{ijt})$. If a truck passes through arc (i, j), the time it arrives at point j is greater than the sum of the service time at point i, the time it arrives at point i, and the travel time from point i to point j (i.e., $t_{jk}^{A} - t_{ik}^{L}$), which can be computed using formulas described in Section 4.1. Constraint (23) traces the arrival time of the private driver at point *j*. Constraint (24) guarantees that the pickup point is serviced before the corresponding delivery point. Constraints (25)-(26) are capacity constraints for trucks and private drivers, respectively. Constraints (27)-(28) track the change of load for each vehicle. Constraint (29) sets the binary decision variables.

5. Solution method

We propose an improved adaptive neighborhood search (ALNS) algorithm for solving GPDP-PD. ALNS was developed inspired by the large neighborhood search (LNS) heuristic proposed by Ropke & Pisinger (2006). The ALNS algorithm, with its simple structure and few parameters involved, is one of the metaheuristic algorithms that have been successfully applied to solve combinatorial optimization problems (Ma et al., 2021; Pralet, 2023; Wolfinger, 2020). Unlike LNS, the destroy and repair operators of ALNS are selected based on their performance in previous iterations. Therefore, ALNS not only retains the benefits of LNS that make it suitable for solving our problem but also searches for a high-quality solution in a shorter time compared to LNS. Moreover, to further enhance ALNS performance, new search strategies together with special operators are designed based on the characteristics of GPDP-PD. The flowchart of the improved ALNS algorithm is shown in Fig. 3. The initial solution s_0 is generated by Insertion Heuristic and assigned to the best solution s_{best} and the current solution $s_{current}$. With a certain probability, a destroy operator and a repair operator are chosen to impose on $s_{current}$ to get a new solution s_{new}. Based on simulated annealing acceptance criteria, when s_{new} is a better solution, s_{new} is accepted as $s_{current}$. Otherwise, we generate $\varepsilon \in [0,1]$ randomly and just accept s_{new} as $s_{current}$ if $e^{-(c(S_{new}) - c(S_{current}))/T} > \varepsilon$. The simulated annealing temperature T needs to be adjusted after each iteration to $T = \kappa T$, where κ is the cooling rate. Finally, the probability of each operator being selected is updated, and this probability is increased when this operator improves the current solution.

The blue boxed section in Fig. 2 shows the innovations of our proposed algorithm. In order for ALNS not to fall into a local optimum, improved search strategies is used. If the current solution $s_{current}$ is not updated during θ_c iterations, a destroy

operator is randomly chosen to get destroyed solution in the next iteration. If the global optimal solution is not updated during θ_g iterations, the temperature T is adjusted to enhance the probability that a worse solution will be accepted ($T = \rho T$). In order to enhance the efficiency of the algorithm, operators are designed according to model characteristics, taking into account not only travel time but also factors such as congestion and vehicle allocation. In addition, the actual traffic conditions need to be taken into account to calculate the fitness function according to the speed calculation methodology in Section 4.1 to more accurately measure the total costs.

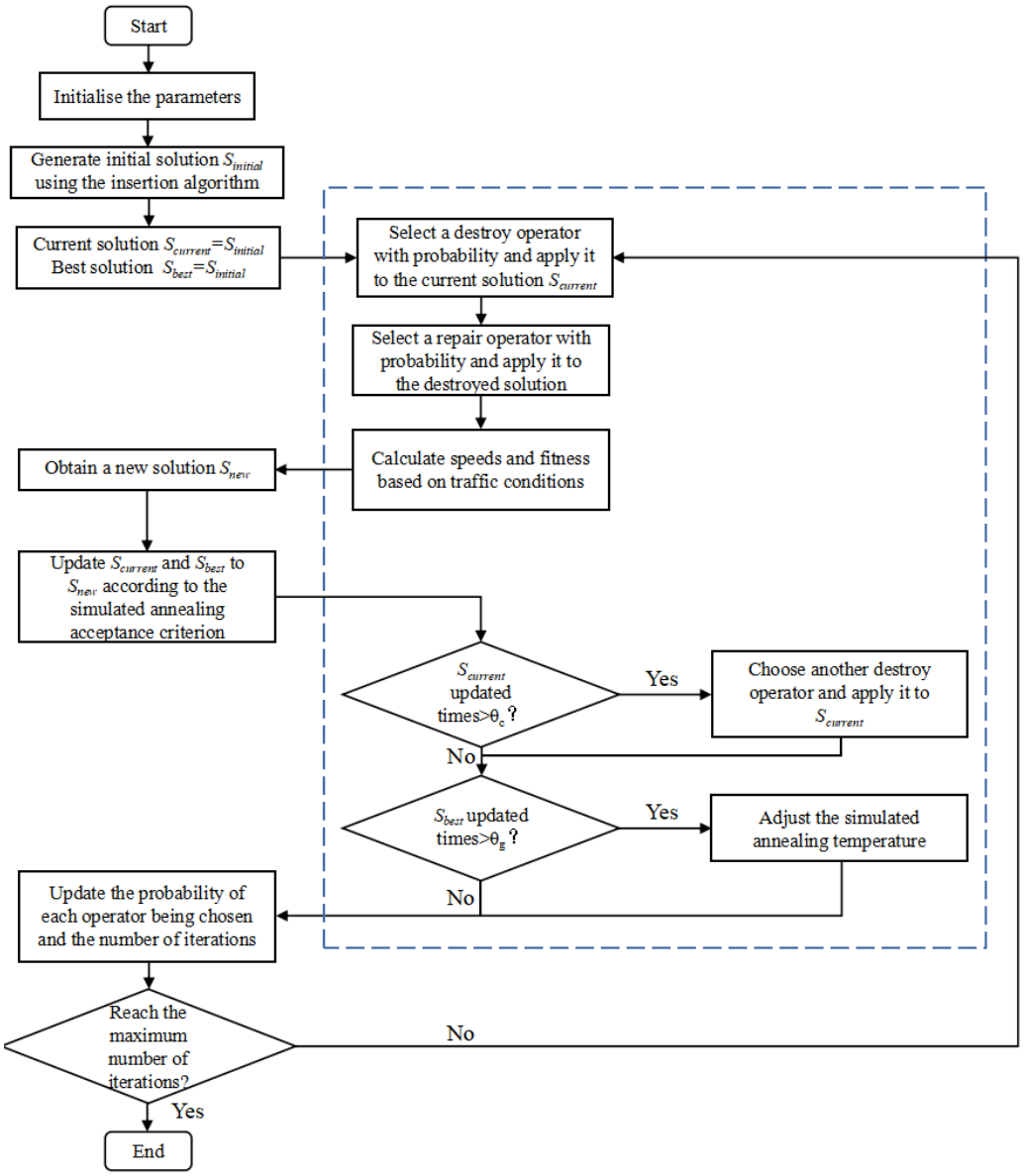

Fig. 2. The flowchart of the improved ALNS.

5.1 Initial solution

Adapted from the method in Ma et al. (2021), an initial solution for GPDP-PD is obtained by the insertion algorithm, and detailed pseudo-code is shown in Algorithm 1. Since both private drivers and trucks may be selected to serve customers, two types of routes need to be constructed: truck routes and private driver routes (lines 3-4). All customers are sequentially inserted in the position that minimizes incremental costs. If a customer is inserted into a feasible location of a company-owned truck route, the insertion cost refers to the increased distance multiplied by the parameter ψ, which is obtained from numerical experiments as 1.05. When all customers have been assigned, the program is terminated, otherwise, it returns to line 5.

Algorithm 1. The pseudo-code of insertion algorithm.

Input: Data of depot, vehicles, customers;
Output: An initial solution S_0

```
Initialize the list of unassigned customers list
Initialize route of the company-owned truck as [0,0]
Initialize route of private driver r as [O(r), D(r)]
While list ≠ ∅
  Select a customer i
  Let n be the number of vehicles and r be the index of a route, r ← 1
  While r ≤ n
    Insert customer i into all possible positions
    Checks if it meets the time and capacity constraints and returns route feasibility (True or False)
    Calculate the insertion cost after inserting customer i
    If Feasibility==False
      Add a large positive number to the increased costs
    End if
    Record all possible insertion locations and the insertion costs
    If r == n and have feasible solutions
      Find a feasible solution with minimal insertion cost
      Update routes and unassigned customer sets list = list \ i
    Else if r == n and There is no feasible solution
      Find a solution with minimal insertion cost
      Update routes and unassigned customer sets list = list \ i
    Else if r < n
      r ← r + 1 ; Return to line 8
    End if
  End while
End while
Output: S0
```

5.2 Adaptive weight adjustment procedure

The adaptive weight adjustment procedure, i.e., roulette wheel mechanism, is applied to select destroy and repair operators. The probability of an operator being selected is updated every I_w iterations according to $P_m^{t+1} = P_m^t(1-\lambda) + \lambda\delta_i / \xi_i$, where λ denotes the roulette wheel parameter, δ_i denotes the score of operator *i*, ξ_i denotes the number of times operator *i* is applied. When operator *i* updates the best solution, it adds θ_1 to its score. When operator *i* gets a better quality solution than the current one, it adds θ_2 to this operator's score. When operator *i* obtains a worse quality solution than the current one, but is accepted, it adds θ_3 to its score and $\theta_1 > \theta_2 > \theta_3$.

5.3 Fitness function

The quality of the solution is evaluated using a fitness function, as shown in Eq. (30). Penalties are increased when the capacity constraint or time limit constraint is violated. The term $r(x)$ denotes the original objective value. $p_q(x)$ denotes the violation of vehicle capacity, and $p_q(x) = \sum_{k=1}^{K}\sum_{i=1}^{n}(F_{it} - Q_T)^+$, where *K* indicates all vehicles, *n* indicates the number of nodes in sub-route, F_{it} indicates to the load on the vehicle t when it leaves point i. $p_t(x)$ refers to whether the time limit is violated, and $p_t(x) = \sum_{r=1}^{R}\sum_{i=1}^{n}(t_{ik}^A - TL_r)^+$, where *R* denotes all private drivers. In addition, the calculation of t_{ik}^A needs to take into account the actual traffic conditions, which are obtained using the method in Section 4.1. ς_1 and ς_2 are penalty coefficients.

$$f(x) = r(x) + \varsigma_1 p_q(x) + \varsigma_2 p_t(x) \tag{30}$$

5.4 Destroy and repair operators

Six destroy operators (D1-D6) and six repair operators (R1-R6) are designed to obtain a new solution. n_d customers need to be removed and $nr_l \le n_d \le nr_u$, where r_l, r_u denote the lower and upper limit of the number of removed customers, n is total

number of customers. The specific description of them is shown below.

Random destroy (D1): n_d customers are selected and removed randomly.

Company-owned route destroy (D2): n_d customers served by company-owned trucks are selected and removed randomly.

Congestion-based destroy (D3): Inspired by the Shaw removal operator (Shaw, 1998), congestion-based destroy operator is designed. A customer *i* is the first point to be randomly selected and removed, and then the next customer to be removed is determined according to the correlation iteratively. The correlation function is $\Delta c(i,j) = \phi_1(d_{ij} + d_{i+n,j+n}) + \phi_2(c_{ij}) + \phi_3(s_{ij})$, where c_{ij} represents whether point *i* and point *j* is originally passed by during congestion. If not, then $c_{ij} = 1$; otherwise, $c_{ij} = -1$. s_{ij} indicates whether *i* and *j* are on the same route. If not, then $s_{ij} = 1$; otherwise, $s_{ij} = -1$. ϕ_1, ϕ_2, ϕ_3 are the weights of different parameters.

Matching-based destroy (D4): The basic process of this operator is the same as D3 but removes customers based on matching level. If point *i* and point *j* are on the same private driver route, the matching level between these two points is $\Delta l = \omega_l \frac{\max\{d_{i,i+n}, d_{j,j+n}\}}{d(r_{od})} + \omega_u \frac{\min\{d_{i,i+n}, d_{j,j+n}\}}{d(r_{od})}$, otherwise, $\Delta l = \lambda(\omega_l \frac{\max\{d_{i,i+n}, d_{j,j+n}\}}{d(r_{ij})} + \omega_u \frac{\min\{d_{i,i+n}, d_{j,j+n}\}}{d(r_{ij})})$. $d(r_{od})$ is the shortest distance connecting origin and destination of the private driver. $d(r_{ij})$ is the shortest distance connecting point *i* and point *j*. λ represents whether *i* and *j* are originally served by the truck. If not, then $\lambda > 1$; otherwise, $\lambda < 1$. ω_l, ω_u are matching parameters, and $\omega_l + \omega_u = 1$.

Worst-distance destroy (D5): The operator removes customers based on the highest distance cost. The distance cost of point *j* is $\Delta c_j = d_{k-1,j} + d_{j,k+1} + d_{o-1,j+n} + d_{j+n,o+1}$, where *k+1*, *o+1* are the points visited after the pickup and delivery points and *k-1*, *o-1* are the points visited before the pickup and delivery points. The point *j* with the largest distance cost should be removed.

Private driver route destroy (D6): This operator removes one or multiple private driver routes. We allow at most pn_r private driver routes to be deleted, where n_r represents the number of private driver routes and $p \in [0.05, 0.20]$.

Random repair (R1): This operator inserts a customer into a position that is randomly selected from the feasible positions in the destroyed solution.

Greedy repair (R2): The increase in insertion cost caused when pickup point *i* and corresponding delivery point *j* are inserted at position *k* is given as follows: $\Delta_{ijk} = \{d_{i-1,i} + d_{i,i+1} - d_{i-1,i+1} + d_{j-1,j} + d_{j,j+1} - d_{j-1,j+1}\}$. Among all feasible positions, points *i* and *j* are inserted into the position that minimizes Δ_{ijk}.

Regret-2 repair (R3): This operator is designed based on greedy repair by introducing a look-ahead mechanism. The insertion position is determined according to the regret value *reg*. $reg = \sum_{j=2}^{K} (f_{cj} - f_{c1})$ denotes the sum of the insertion cost differences for the first *K* best insertion positions, where $K = 2$ and f_{cj} is the *j*th least insertion cost after inserting customer *c*.

Regret-3 repair (R4): This operator is identical to Regret-2 repair except that $K = 3$.

Private driver point-based repair (R5): The operator inserts the point into one of the private driver routes by a simplified cheapest insertion heuristic. If the insertion of customer *c* into any position in the private driver route would cause the capacity or time constraints to be violated, the remaining customers will be inserted into the company-owned truck using Greedy repair.

Private driver route-based repair (R6): The operator inserts the selected point into unused private driver vehicles to construct a new sub-private driver route. If there are no private drivers that can be used, the remaining customers are inserted into the solution using R5.

Three new operators are specially designed according to the characteristics of GPDP-PD. Specifically, operators D3, D4, and R5 are newly-designed. All other destroy and repair operators are inspired by Kitjacharoenchai et al. (2019), Ma et al. (2021), Masmoudi et al. (2018), and Pisinger & Ropke (2005). The third destroy operator is designed to reduce the possibility of vehicles experiencing traffic congestion; the fourth destroy operator is designed to remove customers that deviate from the original travelling schedule or are served by trucks; the fifth repair operator is designed to increase the probability of customers being served by private drivers.

6. Results and discussion

6.1 Test instances

Various datasets are used to test the validity of the ALNS. All experiments are run on a PC with 3.70GHz CPU and 1.60 GHz memory. All instances are solved using CPLEX 12.6 or MATLAB R2021a. All important parameters in the improved ALNS can be found in Table 4.

Table 4
Algorithm parameters definition.

Parameter	Definition	Value
r_l	Lower limit parameter for the number of removed customers	$[0.05, 0.15]$
r_u	Upper limit parameter for the number of removed customers	$[0.12, 0.30]$
$Iter_{\max}$	Maximum number of iterations	800
θ_c	Number of iterations the current solution has not been updated	50
θ_g	Number of iterations the global solution has not been updated	150
T	Initial temperature	100
κ	Cooling rate	0.9989
ρ	Temperature adjustment parameter	1.0006
θ_1	Weight parameter of the operators	25
θ_2	Weight parameter of the operators	23
θ_3	Weight parameter of the operators	8

Dataset S contains 14 small-scale instances for comparison between the improved ANLS and the solver CPLEX to verify the overall performance of ALNS when solving small-scale instances. Customer demand is derived from a survey of parcel delivery quality in China by Zhan et al. (2023). The location data of customers and vehicle origin and destination points are from real road network data in Xi'an City. The largest instance in dataset S is 20 customers and 4 private vehicles.

Dataset L is identical to dataset S but contains 20 medium or large-scale instances consisting of 25-70 customers and 10-30 private drivers. This dataset is used for the case study and sensitivity analysis. The traffic congestion index on 9 May 2023 in Xi'an is selected for our study to describe the vehicle travelling speed of crowd-shipping under congestion. The average traffic congestion index for the Xi'an City is shown in Fig. 3. Fig. 4 shows the distribution of vehicle speeds during peak and off-peak hours in Xi'an as well as the locations of all customers and private drivers.

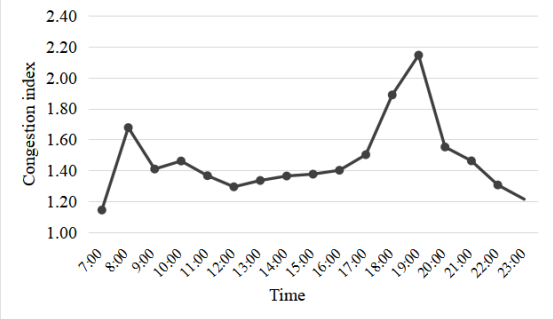

Fig. 3. The average traffic congestion index for Xi'an, 9 May 2023.

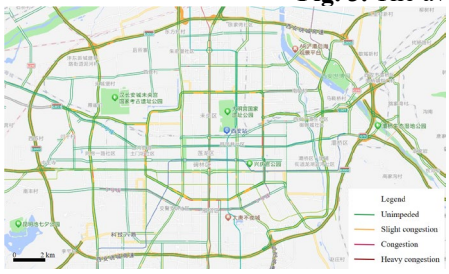

(a)Traffic congestion condition during off-peak hours at major road sections

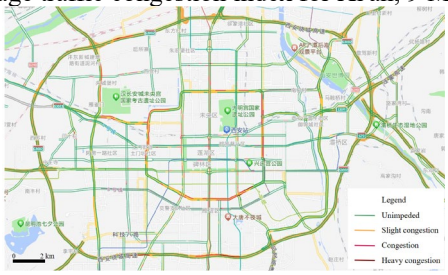

(b) Traffic congestion condition during peak hours at major road sections

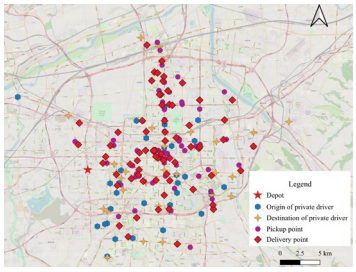

(c) The locations of customers and private drivers

Fig. 4. The distribution of vehicle speeds during peak and off-peak hours in Xi'an as well as the locations of customers and private drivers.

Dataset CMT contains 14 large-scale instances of the pickup and delivery vehicle routing problem, adapted from instances in Kalayci & Kaya (2016). This dataset is mainly used to verify the superiority of ALNS in solving large-scale instances.

6.2 Algorithm performance analysis

To test the performance of the improved ALNS in solving small-sized instances, we compare the CPLEX solver, which can obtain exact solutions, with the improved ALNS solving instances in dataset S. The CPLEX run-time limit is set to 10800 s. Table 5 reports the solutions found by CPLEX within the time limit, the optimal solutions found by improved ALNS, and the time taken to find these solutions. ALNS can find 5 of the same solutions as CPLEX in 8 instances, with a maximum deviation of less than 2%. In addition, improved ALNS can solve larger scale instances than CPLEX, while CPLEX can only solve instances with less than 12 customers in 3 h. As can be seen in Table 5, for all small-scale instances, the improved ALNS algorithm not only leads to the solution quality close to that of CPLEX but also runs in significantly less time compared to CPLEX.

Table 5
Results of the CPLEX and improved ALNS for solving small-scale instances.

Instances	CPLEX	Time (s)	ALNS	Time (s)	Gap (%)
S1-4-2	5.21	1.73	5.21	0.08	0
S2-4-2	7.36	1.58	7.36	0.15	0
S1-6-2	19.20	300.02	19.20	0.41	0
S2-6-2	8.11	8.87	8.11	0.62	0
S1-8-3	13.19	3140.35	13.76	1.44	0
S2-8-3	8.26	5952.28	8.28	1.85	0
S1-10-3	15.49	10593.46	15.81	1.12	1.81
S2-10-3	11.41	112.98	11.41	1.45	0.18
S1-12-3	-	10800	16.90	2.98	-
S2-12-3	-	10800	18.11	2.58	-
S1-15-4	-	10800	13.19	4.45	-
S2-15-4	-	10800	17.51	5.51	-
S1-20-4	-	10800	19.07	9.67	-
S2-20-4	-	10800	26.79	8.11	-

Note: “Gap” denotes the degree of deviation of the solution found by ALNS relative to the solution found by CPLEX; “-”indicates that no solution is found in 3 h

GPDP-PD is an extension and variant of the vehicle routing problem with simultaneous pickup and delivery (VRPSDP). The closest benchmark to the GPDP-PD is the CMT benchmark instances from Kalayci and Kaya (2016). Furthermore, since the improved ALNS we developed is adopted from the classical ALNS, thus the proposed improved ALNS algorithm is compared with two other algorithms: the ant colony algorithm in Kalayci & Kaya (2016) and the classical adaptive large neighborhood algorithm in Ma et al. (2021).

Table 6
Results of the ant colony algorithm, the classical ALNS, and the improved ALNS for solving large-scale instances.

Instances	ACO		CALNS		ALNS			
	Best	Time (s)	Best	Time (s)	Best	Time (s)	Gap (%)	Gap* (%)
CMT1X	466.77	8.50	466.77	9.26	466.77	9.31	0	0
CMT2X	684.21	32.50	684.55	21.14	668.77	22.98	2.26	2.31
CMT3X	721.27	45.20	722.83	40.17	719.32	39.47	0.27	0.49
CMT4X	852.46	142.10	853.15	101.98	853.15	106.04	-0.08	0
CMT5X	1030.55	420.15	1029.25	307.72	1029.25	300.47	0.13	0
CMT6X	555.43	32.50	555.43	17.15	555.43	21.50	0	0
CMT7X	900.12	52.55	900.12	48.77	900.12	48.14	0	0
CMT8X	865.50	120.25	865.50	100.54	865.50	98.36	0	0
CMT9X	1160.68	360.20	1163.52	284.69	1161.37	291.71	-0.06	0.18
CMT10X	1375.77	880.50	1375.46	714.00	1373.40	738.43	0.17	0.15
CMT11X	833.92	42.45	834.12	56.51	834.12	48.91	-0.02	0
CMT12X	662.22	38.25	662.22	47.25	657.59	40.38	0.70	0.70
CMT1Y	466.77	8.50	463.36	8.04	461.21	8.12	1.19	0.46
CMT2Y	684.21	36.50	663.25	20.58	658.50	26.85	3.76	0.72
CMT3Y	721.27	40.30	722.33	39.93	719.00	38.25	3.15	0.46
CMT4Y	852.46	136.35	839.47	117.58	839.47	121.64	15.2	0
CMT5Y	1030.55	410.50	1035.96	309.11	1033.27	312.99	-0.26	0.26
CMT6Y	555.43	32.30	555.43	18.43	555.43	19.87	0	0
CMT7Y	900.12	56.30	901.10	38.87	900.12	40.02	0	1.09
CMT8Y	865.50	127.50	865.50	61.57	865.50	69.19	0	0
CMT9Y	1160.68	350.80	1164.27	288.85	1160.68	284.54	0	0.31
CMT10Y	1373.40	860.25	1373.40	749.04	1373.40	738.08	0	0
CMT11Y	833.92	40.50	833.92	38.02	831.33	38.26	0.31	0.31
CMT12Y	662.22	41.50	663.50	40.84	659.52	41.00	0.41	0.60
Avg.	842.32	179.85	841.27	145.00	839.26	146.02	0.36	0.24

Note: “ACO”=Ant colony algorithm; “CALNS”=Classical adaptive large neighborhood algorithm; “ALNS”=Improved adaptive large neighborhood algorithm; Avg.=Average; “Best” denotes the best solution that can be found; “Gap” and “Gap*” denote the degree of deviation of the solution found by ANLS relative to the solution found in Kalayci & Kaya (2016) and Ma et al. (2021)

Table 6 shows the results of the comparison between the improved ALNS, the ant colony algorithm in Kalayci & Kaya (2016), and the classical ALNS in Ma et al. (2021). The improved ALNS found solutions of the same or better quality than the ACO in 20 out of 24 instances, improving solution quality by an average of 0.36% and reducing solution time by an average of 18.80%. Moreover, although the solution time of the improved ALNS is close to that of ALNS, the improved ALNS found the same or better quality solutions as ALNS in all 24 instances, demonstrating the superiority of the proposed improved ALNS algorithm.

6.3 Case study

6.3.1. Impact of congestion

Road congestion leads to changes in vehicle routes and speeds, which is a key factor in the contradiction between total costs and emissions. Taking S1-6-2 as an example, the vehicle routes during the off-peak and peak hours are shown in Fig. 5, where the vehicle chooses to detour and the truck is activated to serve some customers during the peak hour. Then, Dataset L is used to assess the effect of congestion on costs and emissions in the large network. HCS and LCS denote that the vehicle travels at a constant high speed (55 km/h) and a constant low speed (35 km/h), respectively. VS indicates that vehicle speed is determined by traffic conditions.

Table 7
Comparison of total costs and emissions for HCS, VCS, and VS scenarios

	HCV				LCS				VS				
Instances	Cost	NO_x	PM	FC	Cost	NO_x	PM	FC	Cost	NO_x	PM	FC	Speed
L1-25-10	29.02	412.75	6.93	31.93	47.39	398.79	6.89	29.79	29.97	408.66	6.93	29.77	51
L1-30-10	34.48	632.42	11.31	48.92	72.27	465.14	10.47	37.19	38.02	459.14	10.15	36.06	52
L1-35-15	41.89	742.32	11.08	51.24	57.11	800.32	17.19	57.91	46.21	748.01	11.78	50.45	52
L1-40-15	40.66	828.44	21.02	58.53	71.21	609.94	13.82	45.32	45.36	638.42	12.55	48.42	49
L1-45-20	49.77	857.67	16.13	69.18	101.93	773.46	14.99	61.15	55.10	779.97	15.13	60.31	53
L1-50-20	60.37	1189.12	39.88	70.80	80.99	1209.75	53.43	78.88	66.83	1171.75	38.46	66.56	48
L1-55-25	52.42	1164.65	38.18	77.76	74.58	929.61	35.12	68.19	56.81	1035.52	33.22	70.72	52
L1-60-25	54.57	1211.39	45.16	74.88	155.27	790.26	44.82	47.27	61.11	861.9	38.85	53.90	50
L1-65-30	97.37	1509.64	33.94	108.66	171.19	1542.85	39.69	115.25	102.87	1468.32	33.00	102.86	48
L1-70-30	105.82	1483.63	33.80	108.39	157.85	1586.63	52.46	115.09	110.63	1562.34	40.10	112.39	51
L2-25-10	34.77	556.26	7.29	48.61	51.31	529.31	7.24	45.30	36.60	539.54	7.20	50.71	53
L2-30-10	42.34	760.84	10.59	57.13	66.36	641.92	10.16	56.25	47.08	700.98	9.89	53.72	50
L2-35-15	37.48	362.01	7.51	37.04	52.90	389.54	9.50	40.23	40.68	285.86	4.85	30.62	49
L2-40-15	35.03	238.89	4.07	25.59	54.59	237.27	4.42	25.20	38.98	236.22	3.99	25.30	48
L2-45-20	44.80	325.24	5.54	34.84	61.80	342.48	6.23	36.58	56.20	328.01	5.30	37.42	50
L2-50-20	48.68	277.35	6.02	27.81	79.43	352.18	8.93	29.82	56.26	354.72	9.65	31.88	47
L2-55-25	51.26	360.92	6.14	38.66	87.09	380.14	9.68	43.90	54.58	360.56	6.44	38.70	50
L2-60-25	53.43	495.68	8.03	49.76	77.33	342.2	6.43	36.65	59.22	417.05	7.35	44.67	49
L2-65-30	84.29	495.5	8.46	53.07	113.76	535.55	13.44	60.60	96.32	513.62	9.74	58.97	46
L2-70-30	132.33	1554.52	29.95	114.36	166.52	1879.47	35.46	123.04	124.01	1550.78	29.25	115.14	52
Avg.	56.54	772.96	17.55	59.36	90.04	736.84	20.02	57.68	61.14	721.06	16.69	55.93	50

Note: Cost=Total cost ($); NOx=NOx emissions (g); PM= PM emissions (g); FC=Fuel consumption (L); Speed=Average speed (km/h)

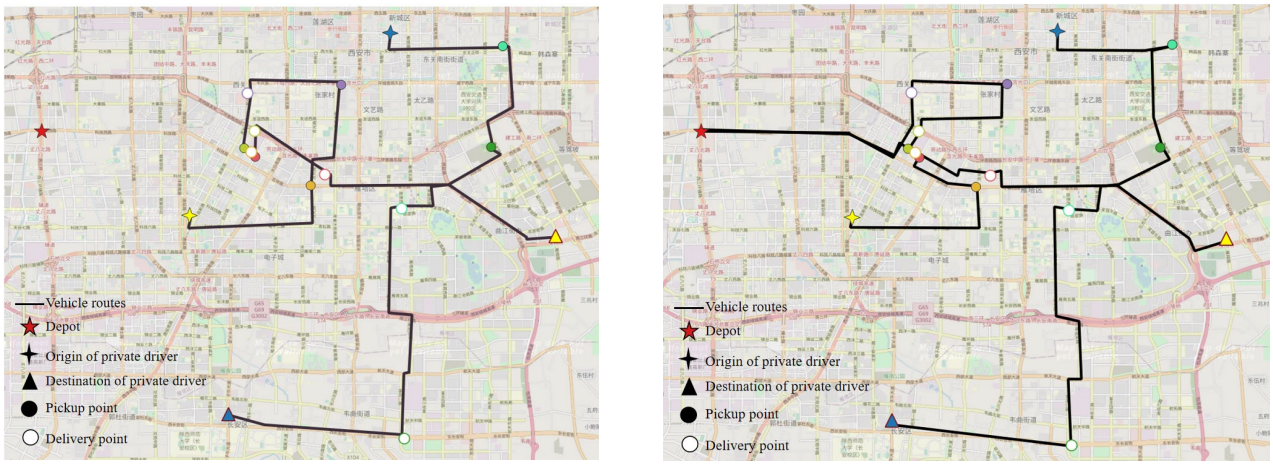

(a) Off-peak vehicle routes (b) Peak vehicle routes

Fig. 5. The vehicle routes during peak and off-peak hours in Xi'an.

Table 7 reports the cost, emissions, and fuel consumption for HCS, VCS, and VS scenarios, respectively. For total costs, it

can be seen that travelling considering traffic congestion increases the cost by 8.14% compared to constant high-speed travelling. These increase in costs stems not only from high transport costs due to low speeds but also from the decreased utilization of cost-saving private drivers. The fact that the cost of travelling at a constant low speed is always the highest also demonstrates that the greater the level of congestion, the higher the costs. Selecting fast travelling speeds during unimpeded periods is cost-effective, but not necessarily environmentally beneficial. From Table 7, compared to travelling at high speeds, congestion leads to slower average vehicle speeds in some instances, resulting in a reduction of 5.78% in fuel consumption, 4.90% in PM, and 6.71% in NO_x. This is due to the fact that when the road is slightly congested, the vehicle is travelling at a speed closer to the economy speed resulting in a decrease in emissions. However, in some cases, there are more emissions from low-speed driving than from congested or even high-speed driving scenarios. This is because when vehicles are travelling at low speeds, as a result of private driver time limits, more private drivers will make detours in order to participate in crowd-shipping, or more environmentally inefficient trucks will be involved in the distribution fleet, resulting in higher emissions. Overall, the environmental benefits of crowd-shipping are closely related to the level of traffic congestion. Whether a crowd-shipping system can help the logistics industry achieve environmental benefits will need to be determined based on the type of vehicles involved in crowd-shipping, the vehicle VMT, and the vehicle speed.

6.3.2. Impact of time limits

In addition to traffic congestion, the time limit for private drivers may also affect the type of vehicles involved in crowd-shipping, the vehicle VMT, and the vehicle speed. The sensitivity analyses of the average results for the instances in the L dataset under different time limits are shown in Fig. 6. From Fig. 6, when the time limit for private drivers is extended, both costs and emissions continue to decrease until the time limit is extended to 0.8 h, at which point both costs and emissions remain stable. The extension of the time limit leads to an increase in both the utilization rate of participating private drivers and the detours of each selected private driver, resulting in lower costs and emissions. When the time limits are extended to a certain point, further extensions will not result in increased detours for private drivers and both costs and emissions will remain stable. It is worth noting that when the time limit is extended from 0.7 h to 0.8 h, the cost decreases while PM and NO_x emissions increase. This is because, while the increase in private driver detours leads to a reduction in emissions during distribution, the decrease in utilization of drivers' original journeys causes an increase in emissions from unused private drivers, resulting in a rise in overall emissions. This implies that companies appropriately encouraging private drivers to extend their time limits may be beneficial to both cost and emission reductions in distribution, but this does not necessarily lead to an overall reduction in emissions. Therefore, the minimization of overall emissions needs to be achieved by regulating the time limits through a comprehensive perspective of the administrators.

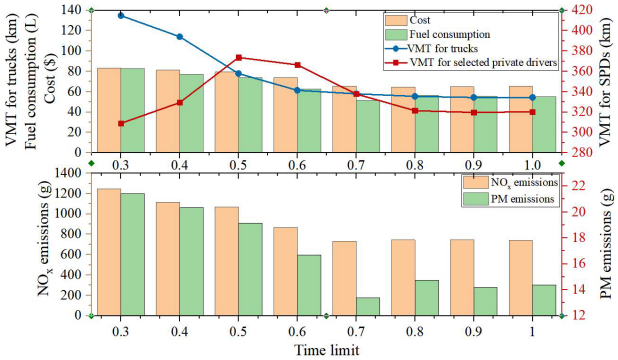

Fig. 6. Comparison of total costs and emissions under different time limits.

Note: "SPDs"=Selected private drivers

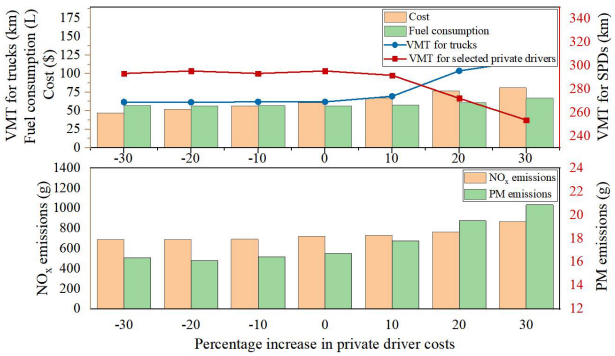

Fig. 7. Comparison of total costs and emissions with different private driver costs.

6.3.3. Impact of private driver costs

The cost of private drivers varies considerably in practice due to factors including supply and demand in the labor market. In this research, a sensitivity analysis is performed to explore the effects of variations in private driver costs in this section, employing three progressively decreasing and three times decreasing private driver costs. The results of these experiments are compared with the base case, and the detailed results can be found in Fig. 7. Fig. 7 shows that any decrease in private driver cost similarly decreases emissions. Compared to the base case, for the case of +10, +20, and +30%, NO_x emissions increased by 1.63, 6.02, and 19.98%, and PM emissions increased by 6.40, 16.50, and 24.54%, respectively. The total costs are increased by 10.39, 25.92, and 32.28%, respectively. Correspondingly, for the cases of -10, -20, and -30%, the total costs are decreased by 7.57, 15.01, and 23.08%, respectively, with little change in emission or energy reductions. As the cost of private drivers rises, the cost-effectiveness of private drivers diminishes, the likelihood of using trucks for distribution rises, and private driver utilization decreases, leading to higher costs and emissions. Further, when the cost of private drivers falls to a certain level, private driver utilization reaches its maximum level. In this regard, while emissions will continue to decrease as private driver costs decrease, the magnitude of the decrease will gradually slow down. In addition, the magnitude of change in PM is larger relative to that of NO_x due to the fact that non-exhaust emissions are more sensitive to vehicle type, and most PM

emissions originate from non-exhaust sources (Liu et al., 2022; Scerri et al., 2023).

7. Conclusions

As the result of increasing distribution activity and customers' expectations for flexible and sustainable distribution services, crowd-shipping has emerged to utilize idle capacity resources in society and is widely regarded as an effective means to enhance sustainable economic development. With the aim of cutting down on NO_x and PM emissions while minimizing distribution costs under traffic congestion conditions, we propose a new integrated model of Green Pickup and Delivery Problem with Private Drivers (GPDP-PD). Our contribution lies in the integration of the exhaust and non-exhaust emission model as well as varying speed into the optimization of customer allocation and vehicle routing in crowd-shipping. In GPDP-PD, a comprehensive objective function for transport and emission costs is considered. In particular, NO_x and exhaust PM emissions related to fuel consumption, as well as non-exhaust PM emissions related to distance travelled are included in our objective function. In order to simulate real-world situations, the two types of traffic conditions (congested and unimpeded) are considered separately. The congestion index is introduced to describe the road congestion level, while the triangular distribution is used to model the variation of vehicle speeds in the case of an unimpeded condition.

To solve the GPDP-PD, we propose an improved adaptive large neighborhood search (ALNS) algorithm incorporating six destroy operators and six repair operators. This improved ALNS algorithm introduces new search strategies to prevent the algorithm from falling into a local optimum. Several operators are designed according to the characteristics of the model to find the optimal solution quickly. A comparison of the solutions obtained by the improved ALNS with the results of CPLEX, the classical ALNS, and the solutions provided by Kalayci and Kaya (2016) reveals that our algorithm can obtain high-quality solutions in a reasonable time. A case study is carried out to provide some useful insights. The results show that vehicle speed, vehicle type, and VMT all influence PM and NO_x emissions, leading to a high degree of uncertainty about the environmental benefits of crowd-shipping under congestion. In particular, a slight reduction in speed for private drivers with appropriate detours is the most environmentally beneficial case. In addition, a time limit of 0.7-0.8 h and a low private driver cost is favorable to achieving environmental and economic benefits at the same time.

Future research on crowd-shipping can be carried out from the following two aspects. (1) One trend is to further approximate the problem to the reality of logistics companies by incorporating other practical requirements, such as compensation pricing for private drivers, time windows, and cargo stability. (2) Other factors such as customer satisfaction can be considered in the model objectives and multi-objective optimization algorithms can be developed to seek Pareto solutions.

References

Archetti, C., Savelsbergh, M., & Speranza, M. G. (2016). The vehicle routing problem with occasional drivers. *European Journal of Operational Research*, *254*, 472-480. https://doi.org/10.1016/j.ejor.2016.03.049

Archetti, C., Guerriero. F., & Macrina, G. (2021). The online vehicle routing problem with occasional drivers. *Computers & Operations Research*, *127*, 105144. https://doi.org/10.1016/j.cor.2020.105144

Barth, M., Younglove, T., & Scora, G. (2005). Development of a heavy-duty diesel modal emissions and fuel consumption model. Tech. rep. UC Berkeley: Research report California Partners for Advanced Transit and Highways (PATH).

Bektas, T., & Laporte, G. (2011). The pollution-routing problem. *Transportation Research Part B: Methodological*, *45,* 1232-1250. https://doi.org/10.1016/j.trb.2011.02.004

Bortolini, M., Calabrese, F., & Galizia, F. G. (2022). Crowd logistics: a survey of successful applications and implementation potential in northern Italy. *Sustainability*, *14*(24), 16881. https://doi.org/10.3390/su142416881

Boysen, N., Emde, S., & Schwerdfeger, S. (2022). Crowdshipping by employees of distribution centers: Optimization approaches for matching supply and demand. *European Journal of Operational Research*, *296*(2), 539-556. https://doi.org/10.1016/j.ejor.2021.04.002

Chen, J., Liao, W., & Yu, C. (2021). Route optimization for cold chain logistics of front warehouses based on traffic congestion and carbon emission. *Computers & Industrial Engineering*, *161*, 107663. https://doi.org/10.1016/j.cie.2021.107663

Cirovic, G., Pamucar, D., & Bozanic, D. (2014). Green logistic vehicle routing problem: Routing light delivery vehicles in urban areas using a neuro-fuzzy mode. *Expert Systems with Applications*, *41*(9), 4249-4258. https://doi.org/10.1016/j.eswa.2014.01.005

Dahle, L., Andersson, H., Christiansen, M., & Speranza, M. G. (2019). The pickup and delivery problem with time windows and occasional drivers. *Computers & Operations Research*, *109*, 122-133. https://doi.org/10.1016/j.cor.2019.04.023

Ghaderi, H., Tsai, P., Zhang, L., & Moayedikia, A. (2021). An integrated crowdshipping framework for green last mile delivery. *Sustainable Cities and Society*, *78*, 103552. https://doi.org/10.1016/j.scs.2021.103552

Cheng, C., Yang, P., Qi, M., & Rousseau, L. M. (2016). Modeling a green inventory routing problem with a heterogeneous fleet. *Transportation Research Part E: Logistics and Transportation Review*, *97,* 97-112. https://doi.org/10.1016/j.tre.2016.11.001

EMEP. (2013). Road vehicle tyre and brake wear, road surface wear. https://www.eea.europa.eu/publications/emep-eea-guidebook-2013/part-b-sectoral-guidance-chapters/1-eSperanzanergy/1-a-combustion/1-a-3-b-road-tyre/view

EMEP. (2019). Road transport. https://www.eea.europa.eu/publications/emep-eea-guidebook-2019/part-b-sectoral-guidance-chapters/1-energy/1-a-combustion/1-a-3-b-i/view

Grigoratos, T., Mamakos, A., Arndt, M., Lugovyy, D., Anderson, A., Hafenmayer, C., Moisio, M., Vanhanen, J., Frazee, R., Agudelo, C., & Giechaskiel, B. (2023). Characterization of particle number setups for measuring brake particle emissions and comparison with exhaust setups. *Atmosphere*, *14*(1), 103. https://doi.org/10.3390/atmos14010103

Hla, Y. A. A., Othman, M., & Saleh, Y. (2019). Optimising an eco-friendly vehicle routing problem model using regular and occasional drivers integrated with driver behaviour control. *Journal of Cleaner Production*, *234,* 984-1001. https://doi.org/10.1016/j.jclepro.2019.06.156

Ichoua, G. M., & Potvin, J. Y. (2003). Vehicle dispatching with time-dependent travel times. *European Journal of Operational Research*, *144*(2), 379-396. https://doi.org/10.1016/S0377-2217(02)00147-9

Kalayci, C. B., & Kaya, C. (2016). An ant colony system empowered variable neighborhood search algorithm for the vehicle routing problem with simultaneous pickup and delivery. *Expert Systems with Applications*, *956*(66), 163-175. https://doi.org/10.1016/j.eswa.2016.09.017

Kara, I., Kara, B. Y., & Yetis, M. K. (2007). Energy minimizing vehicle routing problem. In: International Conference on Combinatorial Optimization and Applications Springer, pp. 62-71.

Kitjacharoenchai, P., Min, B. C., & Lee, S. (2020). Two echelon vehicle routing problem with drones in last mile delivery. *International Journal of Production Economics*, *225,* 107598. https://doi.org/10.1016/j.ijpe.2019.107598

Le, T. V., Stathopoulos, A., Woensel, T. V., & Ukkusuri, S. V. (2019). Supply, demand, operations, and management of crowd-shipping services: A review and empirical evidence. *Transportation Research Part C: Emerging Technologies*, *103,* 83-103. https://doi.org/10.1016/j.trc.2019.03.023

Liu, Y., Chen, H., Li, Y., Gao, J., Dave, K., Chen, J., Li, T., & Tu, R. (2022). Exhaust and non-exhaust emissions from conventional and electric vehicles: A comparison of monetary impact values. *Journal of Cleaner Production*, *331*, 129965. https://doi.org/10.1016/j.jclepro.2021.129965

Lou, P., Zhou, Z., & Zeng, Y. (2024). Vehicle routing problem with time windows and carbon emissions: a case study in logistics distribution. *Environmental Science and Pollution Research*, *31*(11), 16177-16187. https://doi.org/10.1007/s11356-024-31927-9

Ma, B., Hu, D., Chen, X., Wang, Y., & Wu, X. (2021). The vehicle routing problem with speed optimization for shared autonomous electric vehicles service. *Computers & Industrial Engineering*, *161*(8), 107614. https://doi.org/10.1016/j.cie.2021.107614

Macrina, G., Pugliese, L. D. P., & Guerriero, F. (2020). Crowd-shipping: a new efficient and eco-friendly delivery strategycrowdsourced delivery—a dynamic pickup and delivery problem with ad hoc drivers. *Procedia Manufacturing*, *42*, 483-487. https://doi.org/10.1016/j.promfg.2020.02.048

Masmoudi, M. A., Hosny, M., Demir, E., Genikomsakis, K. N., & Cheikhrouhou, N. (2018). The dial-a-ride problem with electric vehicles and battery swapping stations. *Transportation Research Part E: Logistics and Transportation Review*, *118*, 392-420. https://doi.org/10.1016/j.tre.2018.08.005

Meyer, M., & Dallmann, T. (2022). Air quality and health impacts of diesel truck emissions in New York City and policy implications. https://www.trueinitiative.org/media/792240/true-nyc-report-fv.pdf

Michiels, H., Mayeres, I., Panis, I. L., Nocker, L. D., Deutsch, F., & Lefebvre, W. (2012). $PM_{2.5}$ and NO_x from traffic: Human health impacts, external costs and policy implications from the Belgian perspective. *Transportation Research Part D: Transport and Environment*, *17*(8), 569-577. https://doi.org/10.1016/j.trd.2012.07.001

Niu, Y., Yang, Z., Chen, P., & Xiao, J. (2018). Optimizing the green open vehicle routing problem with time windows by minimizing comprehensive routing cost. *Journal of Cleaner Production*, *171,* 962-971. https://doi.org/10.1016/j.jclepro.2017.10.001

Peng, S., Park, W., Eltoukhy, A. E., & Xu, M. (2024). Outsourcing service price for crowd-shipping based on on-demand mobility services. *Transportation Research Part E: Logistics and Transportation Review*, *193*, 103451. https://doi.org/10.1016/j.tre.2024.103451

Pisinger, D., & Ropke, S. (2007). A general heuristic for vehicle routing problems. *Computers & Operations Research*, *34*(8), 2403-2435. https://doi.org/10.1016/j.cor.2005.09.012

Poonthalir, G., & Nadarajan, R. (2018). A Fuel Efficient Green Vehicle Routing Problem with varying speed constraint (F-GVRP). *Expert Systems with Applications*, 100, 131-144. https://doi.org/10.1016/j.eswa.2018.01.052

Pralet, C. (2023). Iterated maximum large neighborhood search for the traveling salesman problem with time windows and its time-dependent version. *Computers & Operations Research*, *150*, 106078. https://doi.org/10.1016/j.cor.2022.106078

Punel, A., & Stathopoulos, A. (2017). Modeling the acceptability of crowdsourced goods deliveries: Role of context and experience effects. *Transportation Research Part E: Logistics Transportation Review*, *105,* 18-38. https://doi.org/10.1016/j.tre.2017.06.007

Rafael, A., Roel, G., & Wouter, D. (2023). Strategic multi-echelon and cross-modal CO_2 emissions calculation in parcel distribution networks: first step toward a common language. *Transportation Research Record*, *2677*(6), 620-630. 10.1177/03611981221149431

Rexeis, M., & Hausberger, S. (2009). Trend of vehicle emission levels until 2020- Prognosis based on current vehicle measurements and future emission legislation. *Atmospheric Environment*, *43*, 4689-4698. https://doi.org/10.1016/j.atmosenv.2008.09.034

Ropke, S., & Pisinger, D. (2006). An adaptive large neighborhood search heuristic for the pickup and delivery problem with time windows. *Transportation Science*, *40*(4), 455-472. https://doi.org/10.1016/j.cor.2016.01.018

Scerri, M. M., Weinbruch, S., Delmaire, G., Mercieca, N., Nolle, M., Prati, P., & Massabò, D. (2023). Exhaust and non-exhaust contributions from road transport to PM10 at a Southern European traffic site. *Environmental Pollution*, *316*, 120569. https://doi.org/10.1016/j.envpol.2022.120569

Shaw, P. (1998). Using constraint programming and local search methods to solve vehicle routing problems. International conference on principles and practice of constraint programming, Springer, Berlin, Heidelberg, pp. 417-431, 10.1007/3-540-49481-2_30

Shi, Y., Zhou, Y., Ye, W., & Zhao, Q. Q. (2020). A relative robust optimization for a vehicle routing problem with time-window and synchronized visits considering greenhouse gas emissions. *Journal of Cleaner Production*, *275*, 124112. https://doi.org/10.1016/j.jclepro.2020.124112

Su, E., Qin, H., Li, J., & Pan, K. (2023). An exact algorithm for the pickup and delivery problem with crowdsourced bids and transshipment. *Transportation Research Part B: Methodological*, *177,* 102831. https://doi.org/10.1016/j.trb.2023.102831

Tao, Y., Zhou, H., & Lai, X. (2023). The pickup and delivery problem with multiple depots and dynamic occasional drivers in crowdshipping delivery. *Computers & Industrial Engineering*, *182*, 109440. https://doi.org/10.1016/j.cie.2023.109440

Timmers, V. R. J. H., & Achten, P. A. J. (2016). Non-exhaust PM emissions from electric vehicles. *Atmospheric Environment*, *134*, 10-17. https://doi.org/10.1016/j.atmosenv.2016.03.017

Wolfinger, D. (2020). A large neighborhood search for the pickup and delivery problem with time windows, split loads and transshipments. *Computers & Operations Research*, *126*, 105110. https://doi.org/10.1016/j.cor.2020.105110

Wu, F., & Dong, M. (2023). Eco-routing problem for the delivery of perishable products. *Computers & Operations Research*, *154*, 106198. https://doi.org/10.1016/j.cor.2023.106198

Yao, K., Yang, B., & Zhu, X. (2019). Low-carbon vehicle routing problem based on realtime traffic conditions. *Computer Engineering and Applications*, *55*(03), 231-237. http://cea.ceaj.org/EN/Y2019/V55/I3/231

Zhan, X., Szeto, W., & Wang, Y. (2023). The ride-hailing sharing problem with parcel transportation. *Transportation Research Part E: Logistics Transportation Review*, *172*, 1033073. https://doi.org/10.1016/j.tre.2023.103073